Electron Densities from Gas-Phase Electron Diffraction Intensities. II. Molecular Hartree–Fock Cross Sections*

D. A. KOHL† AND L. S. BARTELL

Department of Chemistry and Institute of Science and Technology, The University of Michigan, Ann Arbor, Michigan 48104

(Received 17 December 1968)

Differential cross sections for electron scattering based on molecular Hartree–Fock electron densities are compared with cross sections based on the independent-atom approximation for the molecules C_2, N_2, O_2, F_2, and CO. The results show that bonding effects on the electron density manifest themselves to the extent of several percent in the scattered intensity at small scattering angles. Furthermore, molecule-to-molecule variations in the shifts of electron density are clearly reflected in variations in the functional form of the scattered intensity. A comparison of the calculated intensities for N_2 and O_2 with preliminary experimental intensities suggests that electron scattering techniques now in development should be able to provide information about bonding and electron correlation effects competitive in accuracy with that of current quantum-mechanical calculations.

INTRODUCTION

In the preceding paper[1] it was shown that, subject to certain limitations, information about the electron density of molecules can be obtained from gas-phase electron diffraction intensities. The formal treatment of Paper I examined the problem of uniqueness and deferred the question as to whether practical information could be derived from existing experimental techniques. We shall attempt to answer this question in the present paper by calculating differential cross sections for a series of diatomic molecules. The sensitivity of the diffraction approach will be gauged from a comparison of results for Hartree–Fock molecules with results for hypothetical molecules built up of independent Hartree–Fock atoms. Such a comparison not only gives a reasonable assessment of the diagnostic capacity of scattered intensities for bonding effects but it also provides useful guidelines in the selection of analytical representations for electron densities in molecules. Such representations will be indispensable in the transformation of experimental intensities into three-dimensional electron distributions.

THEORY

In Paper I, the function $\sigma_{\rm tot}(s)$ was introduced which represents the electronic contribution to the total scattered intensity for electrons. Furthermore, $\sigma_{\rm tot}(s)$ was subdivided into two components $\sigma_{\rm ne}(s)$ and $\sigma_{\rm ee}(s)$ where, for a diatomic molecule A–B,

$$\sigma_{\rm ne}(s) = -2\left\langle \int \mathbf{dr} j_0(sr)[Z_{\rm A}\rho(\mathbf{r}) + Z_{\rm B}\rho(\mathbf{r}+\mathbf{r}_{\rm AB})]\right\rangle_{\rm vib} \tag{1}$$

$$\sigma_{\rm ee}(s) = \left\langle \int_0^\infty dr j_0(sr) P(r)\right\rangle_{\rm vib}, \tag{2}$$

and

$$\sigma_{\rm tot}(s) = \sigma_{\rm ne}(s) + \sigma_{\rm ee}(s). \tag{3}$$

In Eqs. (1)–(3), s is the scattering variable, $j_0(x)$ is the zeroth-order spherical Bessel function, $Z_{\rm A}$ and $Z_{\rm B}$ are the nuclear charges, and $\langle\ \rangle_{\rm vib}$ denotes vibrational averaging. Nucleus A has been chosen as the origin of the coordinate system, and the position of nucleus B is given by the vector $\mathbf{r}_{\rm AB}$. The functions $\rho(\mathbf{r})$ and $P(r)$ are the electron density and the radial electron–electron distribution, respectively. If the total intensity is separated into elastic and inelastic components, the electronic contribution to the elastically scattered intensity, $\sigma_{\rm elast}(s)$, can be expressed as[2]

$$\sigma_{\rm elast}(s) = \sigma_{\rm ne}(s) + \left\langle \int \mathbf{dr} j_0(sr) \int \mathbf{dr}'\rho(\mathbf{r}')\rho(\mathbf{r}+\mathbf{r}')\right\rangle_{\rm vib}. \tag{4}$$

Since the emphasis in this paper is on the influence of bonding effects, we shall be concerned with difference functions $\Delta\sigma_{\rm tot}(s)$, $\Delta\sigma_{\rm ne}(s)$, and $\Delta\sigma_{\rm elast}(s)$ which are of the form

$$\Delta\sigma(s) = \sigma(s) - \sigma^{\rm iam}(s). \tag{5}$$

The reference function $\sigma^{\rm iam}(s)$ shall be calculated according to the independent-atom approximation for Hartree–Fock atoms, and $\sigma(s)$ represents the exact value of the particular electronic contribution to the scattered intensity. An explicit definition of $\Delta\sigma_{\rm ne}(s)$ is

$$\Delta\sigma_{\rm ne}(s) = \sigma_{\rm ne}(s) - \sigma_{\rm ne}{}^{\rm iam}(s) \tag{6a}$$

$$= -2\left\langle \int \mathbf{dr} j_0(sr)[Z_{\rm A}\Delta\rho(\mathbf{r}) + Z_{\rm B}\Delta\rho(\mathbf{r}+\mathbf{r}_{\rm AB})]\right\rangle_{\rm vib}, \tag{6b}$$

where $\Delta\rho(\mathbf{r})$ is the Roux function,[3] the function cor-

* This research was supported by a grant from the National Science Foundation.

† Present address: Department of Chemistry, The University of Texas at Austin, Austin, Tex. 78712.

[1] D. A. Kohl and L. S. Bartell, J. Chem. Phys. 51, 2891 (1969), Paper I.

[2] R. A. Bonham, J. Phys. Chem. 71, 856 (1967).

[3] M. Roux, S. Besnainou, and R. Daudel, J. Chim. Phys. 54, 218 (1956); M. Roux, M. Cornille, and L. Burnelle, J. Chem. Phys. 37, 933 (1962).

responding to the difference between the molecular electron density and the sum of the densities of the free atoms separated by the distance r_{AB}. For atoms which are aspherical in their ground state by virtue of incompletely filled shells, $\Delta\rho(\mathbf{r})$ can be defined in different ways. To be consistent with the conventional diffraction usage of the independent-atom approximation, we shall adopt the spherical average of the atomic electron density in defining $\Delta\rho(\mathbf{r})$.

An invaluable aid in the discussion of bonding effects on the scattered intensity is the relationship between the average potential energy $\bar{U}$ of the scatterer and the total intensity. It can be shown that $\Delta\bar{U}$, the difference in potential energy between the actual molecule and the reference state (the independent-atom molecule) is given by[2]

$$\Delta\bar{U}=\frac{a_0}{\pi}\int_0^\infty ds\Delta\sigma_{\mathrm{tot}}(s), \tag{7}$$

where the potential energy is in atomic units, a_0 is the Bohr radius in angstroms, and s is given in (angstroms)$^{-1}$. Although the reference state does not correspond to a proper molecular wavefunction, its potential energy is well defined and can be calculated exactly. The potential energy of the real molecule can be obtained, with the aid of the virial theorem, from spectroscopic measurements of the total energy.

Roux functions for all the molecules considered were obtained from Bader[4] in tabulated form and then were fitted by least squares with the functional form

$$\Delta\rho(\mathbf{r})=\Delta\rho(r,\theta)=\sum_n\sum_{k\geq n-1}a_{nk}r^k\exp(-\lambda_{nk}r)P_n(\cos\theta)+\sum_n\sum_{k\geq n-1}b_{nk}(r')^k\exp(-\gamma_{nk}r')P_n(\cos\theta'), \tag{8}$$

where $P_n(x)$ is the Legendre polynomial of degree n, nucleus A is the origin of the coordinate system,

$$r'=(r^2+r_{AB}^2-2rr_{AB}\cos\theta)^{1/2},$$

$$r=(r'^2+r_{AB}^2-2r'r_{AB}\cos\theta')^{1/2},$$

and a_{nk}, λ_{nk}, b_{nk}, γ_{nk} are adjustable parameters. For a homonuclear diatomic molecule, symmetry requires that $a_{nk}=b_{nk}$ and $\lambda_{nk}=\gamma_{nk}$. Since the volume integral over all space of the electron density is equal to the number of electrons, the volume integral of $\Delta\rho(r)$ must equal zero. Expressions for evaluating $\Delta\sigma_{\mathrm{ne}}(s)$ and $\Delta\sigma_{\mathrm{elast}}(s)$ in terms of this representation are given in the Appendix. Because the molecular electron–electron charge distribution has not yet been computed from the Hartree–Fock wavefunctions (and because it would necessarily be rather poor even if it were computed), $\Delta\sigma_{\mathrm{tot}}(s)$ was not calculated. On the other hand, $\Delta\sigma_{\mathrm{tot}}(s)$ has been measured experimentally for two of the molecules, N_e and O_e, but no experimental data for $\Delta\sigma_{\mathrm{ne}}(s)$ or $\Delta\sigma_{\mathrm{elast}}(s)$ are yet available. In a later section, the resemblance between the calculated values of $\Delta\sigma_{\mathrm{ne}}(s)$ and $\Delta\sigma_{\mathrm{elast}}(s)$ and the experimental values of $\Delta\sigma_{\mathrm{tot}}(s)$ will be discussed.

An average of $\Delta\sigma_{\mathrm{ne}}(s)$ and $\Delta\sigma_{\mathrm{elast}}(s)$ must be taken over the vibrations of the molecule before the functions are directly comparable with experiment. For a rigorous result, the dependency of the Roux function on the internuclear separation would have to be known. Unfortunately, the required vibrationally averaged Hartree–Fock distributions have not been calculated. Nevertheless, it is possible to make an approximate correction for this effect as follows. It may be assumed that the molecules vibrate harmonically with an rms amplitude l, where l is known. If the densities in the vicinity of the nuclei follow the motion of the nuclei, the main effect of the vibration is to introduce the James thermal factor $\exp(-l^2s^2/2)$ into each term containing a spherical Bessel function in the expressions for $\Delta\sigma_{\mathrm{ne}}(s)$ and $\Delta\sigma_{\mathrm{elast}}(s)$.

Although the correction to the intensity could have been obtained directly by integrating the Roux function numerically, the intermediate step of expressing $\Delta\rho(\mathbf{r})$ in terms of Eq. (8) was carried out. This representation has the usual advantages associated with analytical expressions and, in addition, is of a form allowing an approximate correction for vibrational effects to be made. Moreover, as proposed in Paper I, if molecular electron densities could be accurately described by a sufficiently small number of terms in Eq. (8), it would be possible to deduce electron densities from scattering experiments. The number of terms required to represent the Roux functions in this study should indicate the likelihood of success of such a procedure. Another potentially valuable application is as follows: The representation of the Roux function by Eq. (7) subdivides the molecular density into "atomic" parts. With a judicious choice in this subdivision, it may be found that the aspherical character of bonded atoms is approximately transferable from molecule to molecule. The resultant aspherical densities might lead to a significant improvement over the usual independent-atom approximation in scattering theory. Furthermore, the form of $\Delta\rho(\mathbf{r})$ introduced here would provide a mathematically tractable scheme for introducing aspherical scattering factors into the calculation of electron and x-ray diffraction intensities.

RESULTS

The Hartree–Fock Roux functions were fitted by a series of terms, as indicated in Eq. (8), using a least-squares method[5] to obtain the parameters a_{nk} and λ_{nk}. Since the magnitude of the Roux function was largest near the nuclei, initial fittings dealt mainly with

[4] R. F. W. Bader, W. H. Henneker, and Paul E. Cade, J. Chem. Phys. **46**, 3341 (1967).

[5] T. G. Strand, D. A. Kohl, and R. A. Bonham, J. Chem. Phys. **39**, 1307 (1963).

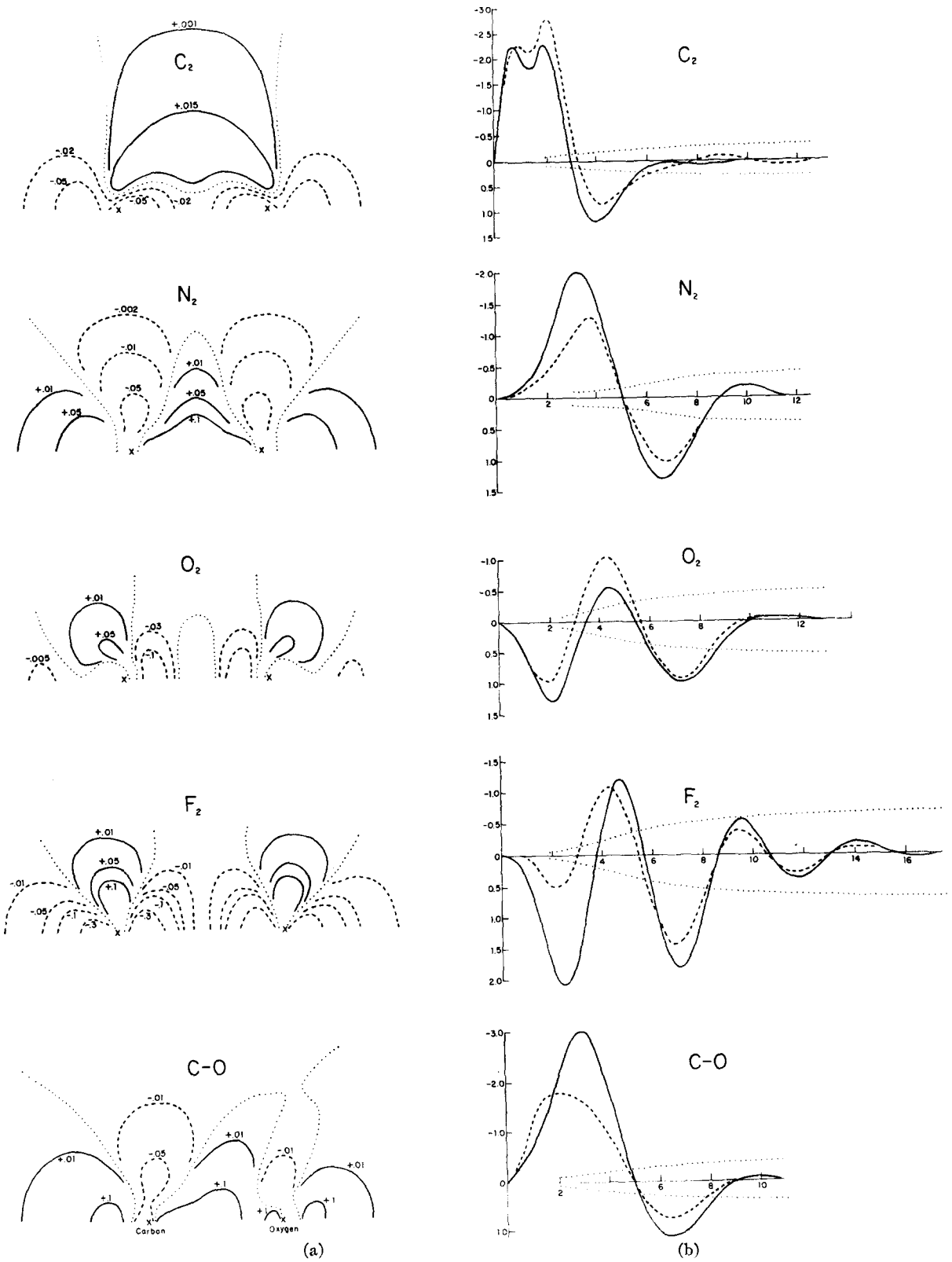

FIG. 1. (a) Roux functions for a series of diatomic molecules. The Roux function or density difference map represents the effect of bond formation on the electron density of the molecule: ——, positive contours in atomic units; – – –, negative contours; • • •, *zero contours*. The positions of the nuclei are identified by ×. (b) The changes in the scattered intensity corresponding to the Roux functions: ——, $\Delta\sigma_{ne}(s)$, the change in the planetary electron–nuclear interference terms; – – –, $\Delta\sigma_{elast}(s)$, the change in the elastic scattering; • • •, 0.5% of the total atomic scattered intensity.

TABLE I. Least-squares parameters for the Roux functions.[a]

	C_2 [b]		N_2 [b]		O_2 [b]		F_2 [b]		CO [c]			
n k	a_{nk} (b_{nk})	λ_{nk} (γ_{nk})	a_{nk} (b_{nk})	λ_{nk} (γ_{nk})	a_{nk} (b_{nk})	λ_{nk} (γ_{nk})	a_{nk} (b_{nk})	λ_{nk} (γ_{nk})	a_{nk}	λ_{nk}	b_{nk}	γ_{nk}
0 0	−1.3336	28.600	−2.7000	11.900	−3.5162	31.446	1.5648	34.269	−3.0389	16.742	−6.5091	30.258
0 1	−25.9884	19.400	29.9022	16.000	−4.3054	7.191	−6.1726	7.662	11.4243	15.258		
0 1	11.5351	11.931	−0.9718	8.053			0.4230	4.823	−1.1383	4.242		
0 1	−2.7036	4.681	−1.9774	4.450								
0 2	4.2841	5.041	3.4446	4.810	2.7062	5.801	6.1306	7.555			−20.5784	9.258
0 2											0.4306	3.242
1 1	−13.6539	16.328	31.6251	39.878	260.0093	18.910	287.6208	20.112	9.6173	31.721	36.9556	35.045
1 1	−1.2985	5.891	71.8363	20.845	−68.3586	9.409	−88.5010	10.717	38.2344	20.136	134.2255	20.791
1 1	1.3500	1.790	−7.2214	7.615			4.7722	8.074	15.6813	15.336	−22.7448	8.661
1 1			0.4814	3.870			−3.3745	6.000	−2.9792	5.441	−1.7061	6.023
1 2					−2.1042	5.039	−12.9149	6.465			10.2672	5.194
1 2					23.0654	6.952	8.5465	5.297				
1 3	−2.2272	2.720										
2 1	−3.9178	11.499	15.8709	29.878	13.1902	16.480	34.6102	25.087	−5.3441	13.676	9.0627	5.111
2 1			−25.3648	14.574	−15.6631	8.980	−81.3146	8.079	9.5424	3.943		
2 1			7.9955	9.394	−5.7056	7.800	−7.4240	6.483				
2 1			13.4487	4.765								
2 2	−68.0394	9.600			1.3500	4.485	−170.7564	10.596				
2 2							7.1850	5.379				
3 3	−11.3424	6.300	15.1373	6.150	64.1155	6.650	16.3245	5.664	12.8231	5.000	10.7984	6.000

[a] Parameters are defined by Eq. (8) of the text for r and r' given in angstroms and the units of the Roux functions are electrons per cubic angstrom. The Roux functions can be converted to atomic units by dividing by 6.749.

[b] The symmetry of homonuclear diatomic molecules requires $b_{nk}=a_{nk}$ and $\gamma_{nk}=\lambda_{nk}$ in Eq. (8).

[c] The origin of the coordinate system is at the carbon nucleus.

this region. Gradually, points at larger radii were added and additional adjustable parameters were introduced. About 1300 points were included, in all, to ensure that $\Delta\rho(\mathbf{r})$ was well characterized. The normalization condition was not imposed until the final stages. Final parameters are listed in Table I. The extreme asymmetry of the Roux function near the nuclei made it necessary to employ a relatively large number of parameters (see Fig. 7 of Ref. 4). Approximately one-third of the parameters served only to represent the region within 0.15 Å of the nuclei, although this region makes very little contribution to the scattered intensity. The Roux functions and the calculated values of $\Delta\sigma_{\mathrm{ne}}(s)$ and $\Delta\sigma_{\mathrm{elast}}(s)$ are given in Fig. 1. The magnitude of the correction to the scattered intensity is illustrated in terms of the dotted envelope, the amplitude of which indicates 0.5% of the total atomic or "noninterference" scattered intensity. The goal of current experimental work is to achieve accuracies in the vicinity of 0.1%.

It is difficult to define an appropriate goodness-of-fit criterion in view of the extreme range of variation of the Roux functions in the spatial region of interest. Because the primary purpose in this phase of the study was to obtain $\Delta\sigma_{\mathrm{ne}}(s)$ rather than to obtain an exact fit of $\Delta\rho(\mathbf{r})$, the accuracy of the calculated values of $\Delta\sigma_{\mathrm{ne}}(s)$ was selected as the primary criterion. The error in $\Delta\sigma_{\mathrm{ne}}(s)$ was determined at various stages in the least-squares refinement by numerically integrating Eq. (6b) using the residuals between the $\Delta\rho(\mathbf{r})$ given by Bader *et al.*[4] and the $\Delta\rho(\mathbf{r})$ given by Eq. (8) to determine the residuals in $\Delta\sigma_{\mathrm{ne}}(s)$. The final values of $\Delta\sigma_{\mathrm{ne}}(s)$ and $\Delta\sigma_{\mathrm{elast}}(s)$ plotted in Fig. 1 represent a blend of purely analytical results with corrections from the numerical integration. Some judgment had to be used in the application of the corrections because the numerical integration was affected by the finite range of integration for small s values and by the finite grid spacing for large s values. The normalization condition on $\Delta\rho(\mathbf{r})$ requiring that $\Delta\sigma_{\mathrm{ne}}(s)$ be zero at $s=0$ provided a means of judging the accuracy of the numerical integration. Except for small s values, $s\leq 2$ Å^{-1}, the peak values of $\Delta\sigma_{\mathrm{ne}}(s)$ and $\Delta\sigma_{\mathrm{elast}}(s)$ given by the analytical expressions are accurate to about 10%. Between $s=0.5$ and $s=2$, it was necessary to rely on the corrections indicated by the numerical integration. The Roux functions at large radii may prove to be appreciably influenced by the vibrations of the nuclei, an effect which has been neglected in these calculations. Therefore, the error in these regions of the Roux function most troublesome to fit may not be significant. Be that as it may, it is quite apparent that, although a good qualitative representation of $\Delta\rho(\mathbf{r})$ can be made with a small number of terms in Eq. (8), appreciable inaccuracies remain even if a fairly large number of terms is taken. Inasmuch as a convergent least-squares analysis of $\Delta\sigma_{\mathrm{ne}}(s)$ in terms of the transform of Eq. (8) requires that the number of terms be limited, it is likely that deductions about the three-dimensional form of $\Delta\rho(\mathbf{r})$ from experiment will be correspondingly limited.

DISCUSSION

The sine transform which connects $\Delta\sigma_{\mathrm{ne}}(s)$ and $\Delta\rho(\mathbf{r})$ implies a reciprocal relationship between the two functions. A delocalized feature in $\Delta\rho(\mathbf{r})$ [or $\Delta\sigma_{\mathrm{ne}}(s)$] corresponds to a localized feature in $\Delta\sigma_{\mathrm{ne}}(s)$ [or $\Delta\rho(\mathbf{r})$]. Moreover, charge shifts at small (large) radii will result in contributions to $\Delta\sigma_{\mathrm{ne}}(s)$ at large (small) s values. A component of the Roux function of the form $f_n(r)P_n(\cos\theta)$ corresponds to a contribution to $\Delta\sigma_{\mathrm{ne}}(s)$ of the form $g_n(s)[\delta_{n0}+j_n(sr_{\mathrm{AB}})]$. (See the Appendix.) As a consequence of the characteristic lack of nodes in the function $g_n(s)$ in the s range of interest, the nodal pattern of $\Delta\sigma_{\mathrm{ne}}(s)$ is determined by the spherical Bessel functions $j_n(sr_{\mathrm{AB}})$, where r_{AB} is the bond distance. For a bond length of 1.2 Å^{-1}, the first node of $j_n(sr_{\mathrm{AB}})$ occurs at widely separated values of s, namely, 2.6, 3.7, 4.8, and 5.8 Å^{-1} for $n=0$, 1, 2, and 3, respectively. Because of the overriding effect on the intra-atomic over the interatomic contributions in the $n=0$ case, the zeroth-order component in $\Delta\sigma_{\mathrm{ne}}(s)$ has local extrema but it has no nodes. Therefore, each Legendre polynomial corresponds to a distinct nodal pattern in s space. The sensitivity of $\Delta\sigma_{\mathrm{ne}}(s)$ to the details of the Roux functions is apparent from Fig. 1. Variations in the form of $\Delta\rho(\mathbf{r})$ from molecule to molecule are reflected in the variations in $\Delta\sigma_{\mathrm{ne}}(s)$. Examination of each of the $\Delta\sigma_{\mathrm{ne}}(s)$ curves with respect to the 0.5% envelope shows that the bonding effects are appreciable, especially at small s values.

It might be thought that the magnitude of the bonding effects would be reduced if the Roux functions were defined with respect to aspherical valence-state atoms as was done in Ref. 3 rather than with respect to the spherically averaged independent atoms adopted here. This is not necessarily true. The Roux function for F_2, for example, depends strongly upon the choice of the reference function. (Compare Fig. 1 of this paper with Fig. 3 of Ref. 4.) Yet, it appears that the two extremes (valence-state and spherical reference atoms) have entirely comparable magnitudes. Curiously, for F_2, the Roux function for the one reference density is approximately the negative of the Roux function for the other! Obviously, in the case of N_2, the valence-state atoms are spherical, making the alternative reference functions identical. In any event, the spherical-atom reference state is found to be a reasonable one. The shifts of density implied by the Roux functions are large enough to justify the selection of the more convenient reference density.

For all of the molecules, $\Delta\sigma_{\mathrm{ne}}(s)$ is small relative to $s^4 I_{\mathrm{tot}}(s)$, the total scattering function, beyond s values of about 10 Å^{-1}. Even for accurate intensity measurements, the uncertainty in $\Delta\sigma_{\mathrm{ne}}(s)$ would probably equal or exceed $\Delta\sigma_{\mathrm{ne}}(s)$, itself, at the larger

scattering angles. This indicates that the scattered intensities are not sensitive to bonding effects near the nuclei if the small r behavior of the Hartree–Fock Roux functions is representative. Apart from this, the primary limitation on the determination of electron densities is the problem of the uniqueness of the transformation from $\Delta\sigma_{ne}(s)$ to $\Delta\rho(\mathbf{r})$. As was shown in the preceding paper, the basis set of Eq. (8) by no means guarantees a unique transformation. In particular it was shown that any of the terms can be exactly replaced by a sum of spherical terms ($n=0$) without altering $\Delta\sigma_{ne}(s)$. Nevertheless, the nodal behavior of $\Delta\sigma_{ne}(s)$ provides strong clues about the properties of the correct solution of the transformation. If the oscillations in $\Delta\sigma_{ne}(s)$ did not arise from an angular dependency in $\Delta\rho(\mathbf{r})$ identifiable with higher-order $P_n(\cos\theta)$ terms, they would have to be due to an enhanced shell structure around the atoms. In order to investigate whether the model ascribing intensity fluctuations solely to shell structure reveals any telltale deficiencies, let us assume that the calculated function $\Delta\sigma_{ne}(s)$ for F_2 arises from a Roux function, $\Delta\rho_0^*(r, \theta)$, which depends only on terms with $n=0$. The resultant solution, calculated according to the procedure described in the preceding paper, is plotted in Fig. 2 in terms of radial profiles of $\Delta\rho_0^*(r, \theta)$ along the directions $\theta=45^a$, 90^a, and 180^a. Although $\Delta\rho_0^*(r, \theta)$ reproduces the scattered intensity exactly, it is a physically unacceptable solution. For one thing, it corresponds to a negative probability of finding electrons in several regions beyond 1.3 Å. Moreover, it implies an absurdly dense and sharp spherical shell of

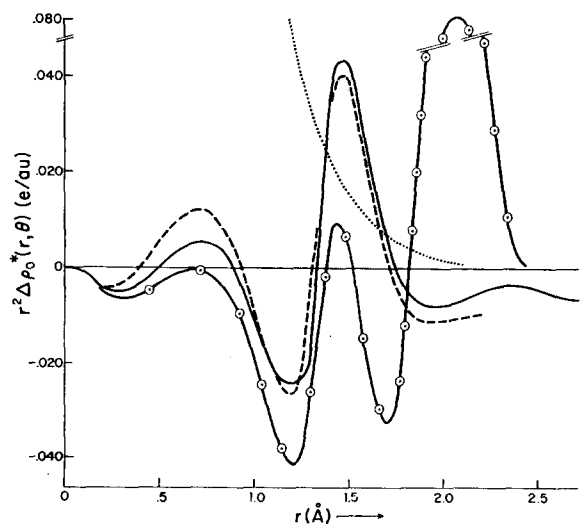

FIG. 2. Radial profiles of $r^2\Delta\rho_0^*(r, \theta)$ for F_2. The Hartree–Fock Roux function and $\Delta\rho_0^*(r, \theta)$, the spherical shell description of the difference in electron density, represent different charge distributions for the molecule F_2 but they produce identical elastically scattered intensities; ——, $\theta=180°$; – – –, $\theta=90°$; OOO, $\theta=45°$. A comparison of the spherical solution with the atomic radial distribution, the dotted line, shows that the spherical-shell description is physically unacceptable.

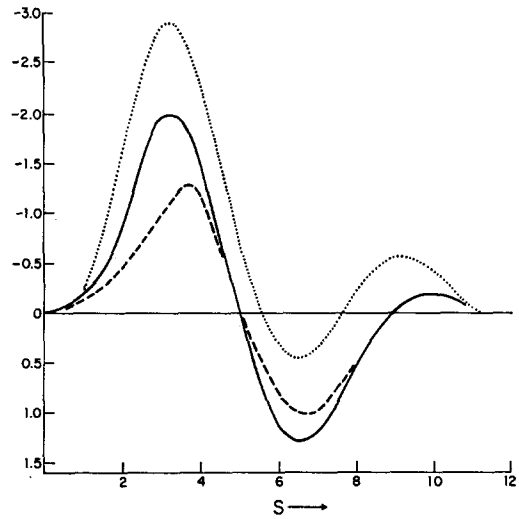

FIG. 3. Bonding and correlation effects on the scattered intensity for N_2. The calculated corrections arising from the bonding effect on the electron density: ——, $\Delta\sigma_{ne}(s)$, the change in the planetary electron–nuclear interference terms; – – –, $\Delta\sigma_{elast}(s)$, the change in the elastic scattering. The dotted curve, $\Delta\sigma_{tot}(s)$, was derived from experimental measurements of the total intensity. Of the three curves illustrated, only the experimental one includes electron-correlation effects as well as one-electron bonding effects.

electrons around each nucleus starting, suspicously, at a radius corresponding to the internuclear separation. The extreme $\Delta\rho_0^*(r, \theta)$ solution, therefore, is easily recognized as spurious. This does not means that the uniqueness of the transformation is not a severe limitation. It does suggest that any dominant contributions to $\Delta\sigma_{ne}(s)$ may be identifiable with the correct Legendre components and semiquantitatively determinable.

Up to this point we have been considering the effect of the electron density, a one-electron property, on the scattered intensity. The total intensity, in its inelastic part, depends also upon the electron–electron distribution function, a two-electron property. For atoms, it is known that Hartree–Fock wavefunctions yield accurate electron densities and that the principal defect of Hartree–Fock wavefunctions is, by definition, their failure to take into account electron correlation effects. For the atoms helium and beryllium, Bartell and Gavin[6] showed that the correlation defect has a very marked influence upon the total intensity even though the error in the Hartree–Fock electron density is negligible. Therefore, the difference between the exact total scattered intensity and the independent-atom total intensity based on Hartree–Fock atoms must depend upon the atomic correlation defect as well as upon the bonding effects on the electron–electron and electron–nuclear distributions. In terms of expressions

[6] L. S. Bartell and R. M. Gavin, Jr., J. Am. Chem. Soc. **86**, 3493 (1964); J. Chem. Phys. **43**, 856 (1965); R. M. Gavin, Jr., and L. S. Bartell, *ibid.* **44**, 3687 (1966); **45**, 4700 (1966).

introduced earlier we can write

$$\Delta\sigma_{\text{tot}}(s) = \Delta\sigma_{\text{elast}}(s) + \Delta\sigma_{\text{inelast}}(s) \quad (9a)$$

$$= [\Delta\sigma_{\text{ne}}(s) + \Delta\sigma_{\text{ee}}{}^{\text{elast}}(s)] + \Delta\sigma_{\text{ee}}{}^{\text{inelast}}(s), \quad (9b)$$

where the inelastic component of the electron–electron function $\Delta\sigma_{\text{ee}}{}^{\text{inelast}}(s)$ manifests the influence of correlation. The practical necessity of adopting an uncorrelated atomic reference function in the derivation of $\Delta\sigma_{\text{tot}}(s)$ from experiment means that $\Delta\sigma_{\text{tot}}(s)$ must tend to exceed $\Delta\sigma_{\text{elast}}(s)$ in the s range where atomic correlation has been found to be important.[6] It is reasonable to expect that both functions, nevertheless, will display the interference effects arising from the structure in the Roux function.

For N_2 and O_2, $\Delta\sigma_{\text{tot}}(s)$ has been measured.[7] As anticipated, the electron–nuclear interference features lead to a similarity in shape between the calculated $\Delta\sigma_{\text{ne}}(s)$ and $\Delta\sigma_{\text{elast}}(s)$ and the experimental $\Delta\sigma_{\text{tot}}(s)$ functions, as is shown in Figs. 3 and 4. Although the experiment represents an admittedly crude attempt to measure bonding effects, it is a successful attempt in several respects. Not only are the interference ripples of $\Delta\sigma_{\text{tot}}(s)$ at least qualitatively correct but so also is the potential energy derived from $\Delta\sigma_{\text{tot}}(s)$ according to Eq. (7). The electron diffraction experiments yield a potential-energy difference between the actual molecule and the independent-atom molecule of -39.2 eV for N_2 and -42.0 eV for O_2. Spectroscopic measurements lead to values of -28.2 and -32.4 eV, respectively, for the same molecules. Although the accuracy of the preliminary diffraction values is not high, it is much higher than the accuracy obtained from a Hartree–Fock molecular wavefunction which gives potential-energy differences of $+3.8$ and $+3.2$ eV. Therefore, even if $\Delta\sigma_{\text{tot}}(s)$ had been calculated with the Hartree–Fock wavefunction for the molecules, quantitative agreement with the experimental curves could not have been expected.

Because of the similarity between the curves for N_2 shown in Fig. 3, it seems improbable that there is any substantial disagreement between the exact one-electron density and the Hartree–Fock electron density. Results for the H_2 molecule, which was studied at the same time as N_2 and O_2, were also in good agreement with calculated values of $\Delta\sigma_{\text{tot}}(s)$, as previously reported.[7] There being no contradictory evidence, it seems likely that the existing measurements of $\Delta\sigma_{\text{tot}}(s)$ capture, qualitatively, the essential features relatable to bonding effects. Current efforts to reduce experimental uncertainties by an order of magnitude look promising. An improvement in accuracy by such a factor would lead to quantitative information on the shifts of electron distribution associated with the formation of bonds.

[7] D. A. Kohl and R. A. Bonham, J. Chem. Phys. **47**, 1634 (1967).

CONCLUSIONS

For many years it has been considered unlikely that useful three-dimensional information on molecular electron densities could be obtained from gas-phase scattered intensities. The results of this paper put the role of electron scattering as a means of studying bonding and correlation effects into a more proper perspective. We have demonstrated that even in molecules more complex than H_2 (a case treated elsewhere[7]) the scattered intensity is measurably sensitive to bonding effects. It is also evident that the amount of information about the electron density which can be derived from vapor-phase experiments is subject to some fundamental limitations. On the other hand, there is no problem of uniqueness in the transformation from $\rho(\mathbf{r})$ to $\sigma_{\text{ne}}(s)$, and the scattered intensity may prove to be more suitable as a test of computed electron densities than as a means for determining densities directly. Most of the accurately measured molecular properties can be represented by a single number. Quantum-mechanical calculations of these properties, with the exception of the total energy, are for the most part not known to represent definite upper or lower bounds. A comparison between calculated and experimental values usually only establishes that the two values agree or disagree. If the two results agree, it may be accidental and the agreement may worsen when an "improved" wavefunction is used for the calculations. The exact scattered intensity cannot be in complete agreement at all scattering angles with a scattered intensity derived from an incorrect wavefunction. Therefore, electron scattering may prove to be one of the best observables in addition to the total energy for determining the quality of computed wavefunctions.

APPENDIX: ANALYTICAL EXPRESSIONS FOR $\sigma_{\text{ne}}(s)$ AND $\sigma_{\text{elast}}(s)$

For the special case of diatomic molecules, the molecular electron density $\rho_M(\mathbf{r})$ has cylindrical symmetry about the internuclear axis. It is assumed that $\rho_M(\mathbf{r})$ can be written as

$$\rho_M(\mathbf{r}) = \rho_A(\mathbf{r}) + \rho_B(\mathbf{r} - \mathbf{r}_{AB}), \quad (A1)$$

where $\mathbf{r}_{AB}$ is the internuclear vector between nucleus A and nucleus B and that $\rho_A(\mathbf{r})$ and $\rho_B(\mathbf{r})$ have the functional form

$$\sum_n P_n(\cos\theta) \sum_k a_{nk} r^k \exp(-\lambda_{nk} r). \quad (A2)$$

First consider $\sigma_{\text{ne}}(s)$, which is given by

$$\sigma_{\text{ne}}(s) = 2Z_A \int \mathbf{dr} j_0(sr)\rho_M(\mathbf{r})$$

$$- 2Z_B \int \mathbf{dr} j_0(sr)\rho_M(\mathbf{r}+\mathbf{r}_{AB}), \quad (A3)$$

where $j_0(x)$ is the zeroth-order spherical Bessel function and $Z_A(Z_B)$ is the nuclear charge on nucleus A(B). The expression given in Paper I for homonuclear diatomic molecules is easily extended to give

$$\sigma_{ne}(s) = -8\pi[Z_A g_0^A(s) + Z_B g_0^B(s) + Z_A \sum_n g_n^B(s) j_n(sr_{AB}) + Z_B \sum_n g_n^A(s) j_n(sr_{AB})], \quad \text{(A4)}$$

where

$$g_n(s) = (2s)^n n! \sum_k a_{nk}(-d/d\lambda_{nk})^{k-n+1}(s^2+\lambda_{nk}^2)^{-n-1}$$

and the superscripts denote which set of parameters is involved. To obtain the expression for $\sigma_{elast}(s)$ it is necessary to evaluate

$$\mathfrak{F}^2(s) = \frac{1}{4\pi}\int d\Omega_s \int \mathbf{dr} \times \exp(i\mathbf{s}\cdot\mathbf{r}) \int \mathbf{dr}'\rho_M(\mathbf{r}')\rho_M(\mathbf{r}+\mathbf{r}'), \quad \text{(A5)}$$

where $\int d\Omega_s$ denotes integration over all orientations of the vector $\mathbf{s}$. Introducing the expression in Eq. (A1) for $\rho_M(\mathbf{r})$ and making numerous substitutions, one obtains

$$\mathfrak{F}^2(s) = \frac{1}{4\pi}\int d\Omega_s[F_{AA}(\mathbf{s}) + F_{BB}(\mathbf{s}) + F_{AB}(\mathbf{s}) + F_{BA}(\mathbf{s})],$$

where

$$F_{AA}(\mathbf{s}) = \int d\mathbf{r}\rho_A(\mathbf{r}) \times \exp(-i\mathbf{s}\cdot\mathbf{r}) \int \mathbf{dy}\rho_A(\mathbf{y}) \exp(i\mathbf{s}\cdot\mathbf{y}),$$

$$F_{BB}(\mathbf{s}) = \int \mathbf{dr}\rho_B(\mathbf{r}) \exp(-i\mathbf{s}\cdot\mathbf{r}) \int \mathbf{dy}\rho_B(\mathbf{y}) \times \exp(i\mathbf{s}\cdot\mathbf{y}),$$

$$F_{AB}(\mathbf{s}) = \exp(i\mathbf{s}\cdot\mathbf{r}_{ab}) \int \mathbf{dr}\rho_A(\mathbf{r}) \times \exp(-i\mathbf{s}\cdot\mathbf{r}) \int \mathbf{dy}\rho_B(\mathbf{y}) \exp(i\mathbf{s}\cdot\mathbf{y}),$$

and

$$F_{BA}(\mathbf{s}) = \exp(-i\mathbf{s}\cdot\mathbf{r}_{ab}) \int \mathbf{dr}\rho_B(\mathbf{r}) \times \exp(-i\mathbf{s}\cdot\mathbf{r}) \int \mathbf{dy}\rho_A(\mathbf{y}) \exp(i\mathbf{s}\cdot\mathbf{y}). \quad \text{(A6)}$$

For the functional form of $\rho_A(\mathbf{r})$ and $\rho_B(\mathbf{r})$ one obtains[8]

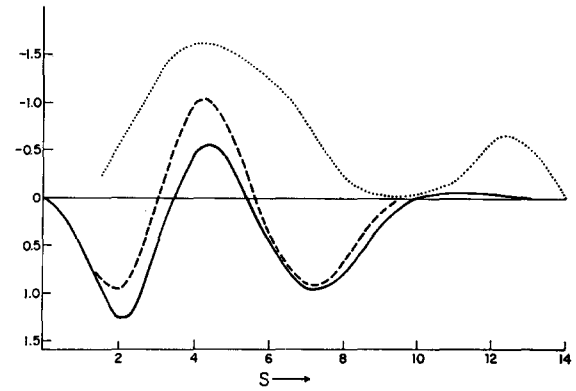

FIG. 4. Bonding and correlation effects on the scattered intensity for O_2. See Fig. 3 for meaning of curves.

$$\int \mathbf{dr}\rho(\mathbf{r}) \exp(ip\mathbf{s}\cdot\mathbf{r}) = 4\pi \sum_n (pi)^n P_n(\cos\theta_s) g_n(s), \quad \text{(A7)}$$

where $p = \pm 1$ and $g_n(s)$ is defined above. The average over all orientations of the terms $F_{AA}(s)$ and $F_{BB}(s)$ gives

$$\frac{1}{4\pi}\int d\Omega_s F_{AA}(\mathbf{s}) = (4\pi)^2 \sum_n (2n+1)^{-1}[g_n^A(s)]^2$$

and

$$\frac{1}{4\pi}\int d\Omega_s F_{BB}(\mathbf{s}) = (4\pi)^2 \sum_n (2n+1)^{-1}[g_n^B(s)]^2. \quad \text{(A8)}$$

The expression for the cross terms reduces to

$$\frac{1}{4\pi}\int d\Omega_s F_{AB}(\mathbf{s}) = 8\pi^2 \sum_n (-i)^n g_n^A(s) \times \sum_m i^m g_m^B(s) \sum_{l=0}^{\infty} (2l+1) i^l j_l(sr_{AB}) P_{nml} \quad \text{(A9)}$$

and

$$\frac{1}{4\pi}\int d\Omega_s F_{BA}(\mathbf{s}) = 8\pi^2 \sum_n i^n g_n^A(s) \sum_m (-i)^m g_m^B(s) \times \sum_{l=0}^{\infty} (2l+1)(-i)^l j_l(sr_{ab}) P_{nml},$$

where

$$P_{nml} = \int dx P_n(x) P_m(x) P_l(x).$$

The function P_{nml} is zero unless the indices form a

[8] M. Abramowitz and I. A. Stegun, *Handbook of Mathematical Functions* (U.S. Government Printing Office, Washington, D.C., 1965), Eq. 10.1.47, p. 440.

triangle whose perimeter is an even number,[9] so that for small values of n and m only a few terms from the infinite sum are nonzero. The final expression for $\sigma_{\text{elast}}(s)$ is given by

$$\sigma_{\text{elast}}(s)=\sigma_{\text{ne}}(s)+\mathfrak{F}^2(s)$$
$$=\sigma_{\text{ne}}(s)+16\pi^2\Big(\sum_n (2n+1)^{-1}\{[g_n{}^{\text{A}}(s)]^2$$
$$+[g_n{}^{\text{B}}(s)]^2\}+\sum_n\sum_m g_n{}^{\text{A}}(s)\,g_m{}^{\text{B}}(s)\sum_{l=0}^{\infty}(2l+1)$$
$$\times j_l(sr_{\text{AB}})i^{n+m+l}(-1)^n P_{nml}\Big). \quad \text{(A10)}$$

With the aid of analytic expressions for atomic electron densities[10] of the form

$$\sum_j A_j e^{-\lambda_j r}/r,$$

it is possible to obtain $\Delta\sigma_{\text{elast}}(s)$ by evaluating Eq. (A10) with and without the parameters for the Roux function.

ACKNOWLEDGMENT

We wish to thank Professor R. F. W. Bader for providing us with the calculated density difference maps for all of the molecules.

[9] A. Erdelyi *et al.*, *Tables of Integral Transforms* (McGraw-Hill Book Co., New York, 1954), Vol. 2, p. 280.

[10] H. L. Cox, Jr., and R. A. Bonham, J. Chem. Phys. **47**, 2599 (1967).

THE JOURNAL OF CHEMICAL PHYSICS VOLUME 51, NUMBER 7 1 OCTOBER 1969

Crystal-Field Spectra of $d^{3,7}$ Ions. V. Tetrahedral Co^{2+} in $ZnAl_2O_4$ Spinel

J. FERGUSON,* D. L. WOOD, AND L. G. VAN UITERT
Bell Telephone Laboratories, Incorporated, Murray Hill, New Jersey 07974
(Received 14 April 1969)

Absorption and fluorescence spectra of Co^{2+} in the tetrahedral (T_d) site of $ZnAl_2O_4$ spinel (gahnite) at low temperatures have been observed and analyzed. The resulting energy-level diagram includes four quartet states and nine doublets, and has been interpreted first in terms of a weak field formalism without spin–orbit coupling. In this analysis the "free-ion" levels for $Dq=0$ were deduced and compared with those for a free ion outside the influence of the crystalline environment. The reduction in the electrostatic interaction parameters F_2 and F_4 in the crystal is due to the effect of covalency. A second approach has been used to analyze the fine structure of the energy levels in terms of a strong field spin–orbit formalism. The fine structure can be explained for all the bands on the basis of simple spin–orbit splitting, but the possibility of a Jahn–Teller distortion of the ${}^4T_{1a}$ state cannot be entirely eliminated.

I. INTRODUCTION

The absorption spectra of tetrahedral Co^{2+} complexes have been studied in varying amounts of detail, both in solutions and in crystals. Crystal spectra are necessary for an analysis of the details of spin–orbit splitting, but in every case, so far, the site symmetry of the Co^{2+} has been less than T_d. The ligand-field analyses have, therefore, been handicapped by the presence of low-symmetry components whose effects cannot readily be separated from the effects of spin–orbit coupling. It is therefore of considerable interest to examine in detail the energy levels of Co^{2+} in an undistorted tetrahedral site. In the present paper we report the absorption and emission spectra of Co^{2+} in $ZnAl_2O_4$, where the tetrahedral site has no distortion, and we give a detailed ligand-field analysis of the results.

II. THEORY

In the first paper of this series[1] the strong-field spin-orbit matrices of Eisenstein[2] were used to analyze the absorption spectra of crystals containing the $CoCl_4^{2-}$ complex ion. The same theory is also used in the present paper to discuss details of the spin–orbit structure of the spin- allowed absorption bands. However, as we have pointed out elsewhere[3] the strong-field matrices are inconvenient for the analysis of the doublet states of Co^{2+} and Cr^{3+} because in the diagonalization of the matrices with $Dq=0$ (the free-ion case) using the electrostatic interaction parameters B and C a good agreement with the observed free-ion levels is not achieved. A much better agreement between observed and calculated free-ion term energies can be obtained by adding a Trees correction to the expressions for the term energies in the weak-field matrix diagonal terms. The remaining discrepancies between theory and experiment can then be ascribed, quite safely, to the effects of configuration interaction which are neglected in our work. Therefore, because the Trees correction can be easily included this way,[3] we chose to make an analysis of the over-all spectrum in terms of a weak-field formalism, based on the matrices of Finkelstein and Van Vleck.[4] It is only because we did

* Present address: National Standards Laboratory, CSIRO, Chippendale, N.S.W., Australia.

[1] J. Ferguson, J. Chem. Phys. **39**, 116 (1963).

[2] J. C. Eisenstein, J. Chem. Phys. **34**, 1628 (1961).

[3] J. Ferguson and D. L. Wood, Mol. Phys. (to be published).

[4] R. Finkelstein and J. H. Van Vleck, J. Chem. Phys. **8**, 790 (1940).